Journal of Applied Polymer Science

Chemorheological time-temperature-transformation-viscosity diagram: Foamed EPDM rubber compound

Nora Catalina Restrepo-Zapata,[1] Ben Eagleburger,[2] Travis Saari,[2] Tim A Osswald,[2] Juan Pablo Hernández-Ortiz[1,3]

[1]Departamento de Materiales y Minerales, Universidad Nacional de Colombia—Medellin, Calle 75 No. 79A-51, Bloque 17, Medellín, Colombia

[2]Department of Mechanical Engineering, Polymer Engineering Center, University of Wisconsin-Madison, 1513 University Avenue, Madison, Wisconsin 53706

[3]Institute for Molecular Engineering, University of Chicago, 5640 South Ellis Avenue, Chicago, Illinois 60637

Correspondence to: J. P. Hernandez-Ortiz (E-mail: jphernandezo@unal.edu.co or jphernandezo@wisc.edu or jphernandezortiz@uchicago.edu)

ABSTRACT: Thermal analysis, rheometry, and kinetic modeling are used to generate a comprehensive processability diagram for thermosetting and elastomeric resins. A chemorheological "time-temperature-transformation-viscosity" diagram is proposed to fully characterize curing reactions toward process' on-line control, optimization, and material design. Differential scanning calorimetry and thermogravimetric techniques are used to measure total reaction heat, degree of vulcanization, and cure kinetics. The viscosity, as a function of temperature and cure degree, is obtained from parallel plate rheometry. The auto-catalytic Kamal–Sourour model, including a diffusion-control mechanism, is used to model cure kinetics, while the Castro–Macosko model serves to model the rheological behavior. Non-linear least-squares regression and numerical integration are used to find models' parameters and to construct the chemorheological diagram. The usefulness of the proposed methodology is illustrated in the context of an industrial-like Ethylene Propylene Diene Termononer rubber compound that includes a chemical blowing agent. Even though the rubber formulation contains crosslinking agents, primary and secondary accelerators, promoters, activators, and processing aids, the chemorheological diagram is obtained consistently, validating the proposed methodology to any thermosetting or elastomeric resin. © 2016 Wiley Periodicals, Inc. J. Appl. Polym. Sci. **2016**, *133*, 43966.

KEYWORDS: crosslinking; elastomers; foams; kinetics; rheology

Received 18 March 2016; accepted 15 May 2016

DOI: 10.1002/app.43966

INTRODUCTION

Rubbers, elastomers, and thermosets are polymeric materials that in the un-cured, or un-vulcanized, state are constituted by independent high-molecular weight molecules. The entanglements between molecules drive the viscoelastic behavior, which, at high temperatures (or long deformation times), result in a non-linear viscous fluid that allows flow and processing.[1–3] These materials solidify by a chemical curing process, called vulcanization, in the rubber community. During cure, additional chemical bonds are created between the independent molecules, thereby creating a three dimensional cross linked network. In most of carbon organics, the extra bonds are formed by breaking double bonds (unsaturations) and forming new covalent and/or ionic bonds between molecules. Sulfur is often used to provide the linkage between molecules due to its chemical valence and atomic size.[4] Thermosetting resins and silicone-based organics require different types of curing agents; however, the aim behind curing is the same: to provide extra chemical bonding between molecules. The chemical crosslinks generated between molecules hinder their relative motion and the ability to undergo plastic deformation.[5] Therefore, to process these materials, deformation and flow, to obtain the desired shape, must be done before curing or vulcanization. Consequently, the final properties and the physical aspect of the product depend on processing (mixing, molding, etc.) and cure quality.

Industrial elastomeric or thermosetting compounds contain, in addition to the curing agent, additives that enhance processability, aid control or provide extra features to the final product. Among them are flame-retardants, plasticizers, reinforcing fibers, and foaming agents. As a result, optimization and control require a detailed knowledge of mixing protocols, processing, curing and materials' properties. All of them, unfortunately, possess complex

and non-linear relationships that are hard to envision. For instance, during rubber processing, multiple variables from the type of process, rubber, additives, mixing, and vulcanization must be considered. A good starting point toward control and optimization is to have the time-temperature-transformation (TTT) diagram of the compound.[1,6] Such a diagram provides a two-dimensional map that guides the proper selection of processing conditions, that is, the "processability window." During the last decade, we had developed a robust experimental and numerical methodology that calculates the TTT diagram of any polymeric resin.[7–12] A natural evolution of such a diagram is to include the rheological information of the compound as a function of time and conversion. We call this the chemorheological Time-Temperature-Transformation-Viscosity (TTT-η) diagram. In this article, we present the methodology, experimental and numerical, that completes our previous scheme to generate the TTT-η diagram.

The chemorheological component is generated from differential scanning calorimeter (DSC) analysis and parallel plate rheometry, followed by numerical modeling for the cure kinetics and the viscosity. The kinetic and the rheological modeling are done using phenomenological descriptions for convenience; however, the proposed methodology is generalizable to any model of preference. It is important to highlight that the chemorheological diagram is intended to provide the processability window to guide optimization and control. A complete platform, for a comprehensive design, will require modeling and simulation, including fluid mechanics, transport, and rheology.[13] However, within the experimental characterization limits (temperatures and rates), the chemorheological diagram gives the required information for the transport equations, including the constitutive behavior and the reaction kinetics.[2,13,14]

We present the TTT-η methodology in the context of an industrial Ethylene Propylene Diene Termononer (EPDM) rubber compound that includes a chemical foaming agent. This particular selection provides an extra challenge to the proposed methodology because, in addition to the rubber compound, there is a parallel blowing reaction that the TTT-η must capture. A successful production of polymeric foams requires proper curing-blowing control, which depends on the delicate balance between the reactions. An additional motivation relies in the fact that the complex interaction between polymeric molecules and additives during processing is not fully understood; therefore, companies that develop these materials use trial and error methodologies to achieve adequate formulations for each specific application. It involves expensive and time-consuming experimental setups that may hinder competitiveness.[15,16] The proposed methodology is then intended to condense all these reactions and interactions in the chemorheological diagram.

EXPERIMENTAL

EPDM Compound

Crystalline and amorphous EPDM rubber provided by DSM® are used with catalyst, accelerators, and process aids. Table I lists the ingredients that constitute the used EPDM compound. The *p*′,*p*-oxybis benzene sulfonyl hydrazide (OBSH) blowing agent is used and provided by Chemtura®.

Table I. Industrial-Like EPDM Compound Formulation in phr (Pounds per Hundred of Rubber)

Ingredient	Quantity (phr)	Function
Crystalline EPDM	75.0	Base elastomer
Amorphous EPDM	25.0	Base elastomer
Carbon black	90.0	Promoter
Zinc stearate	2.0	Processing agent (Releasing agent)
Brown factice	15.0	Promoter
Kaolin	60.0	Activator
Zinc oxide	6.6	Processing agent (Softener)
Naphthenic oil	97.9	Processing agent (Adhesion agent)
Hydrocarbon resin	4.0	Processing agent (Releasing agent)
Polyethylene glycol	2.6	Primary accelerator
MTB[a]	0.7	Primary accelerator
MBTS[b]	2.0	Secondary accelerator
ZDBC[c]	1.5	Secondary accelerator
TMTD[d]	0.6	Secondary accelerator
DPTT[e]	1.2	Secondary accelerator
Ethyl tellurac	0.4	Primary accelerator
Sulfur	2.0	Vulcanizing agent
OBSH	3.0	Blowing agent
Calcium oxide	10.5	Activator

[a] MBT, 2-Mercaptobenzothiazole.
[b] MBTS, Mercaptobenzothiazole disulfide.
[c] ZDBC, Zinc dibutyl dithiocarbamate.
[d] TMTD, Tetramethyl thiuram disulfide.
[e] DPTT, Dipentamethylene thiuram tetrasulfide.

We found that the quality of the TTT-η diagram depends on the consistency of the compound. Thermosetting polymers and silicone rubbers ensure the homogeneous mixing using static mixers and mixing heads in extrusion and injection molding processes.[17,18] Conversely, the mixing on rubber compounds is done by batches and it must be controlled step-by-step to ensure reproducibility. In this work, the mixing is done at room temperature using a mill mixer. First, the EPDM rubber is placed in the mill until the viscosity decreases to facilitate the incorporation of solid compounds. Fillers and process aids are included and cuts are made in the rubber to ensure distributive mixing. The mixture is stabilized at room temperature for five days and then mixed again adding the vulcanization and foaming agents. A final stabilization stage is done for 20 h before processing and/or characterization analysis. The torque rheometry data are shown in Figure 1, where a typical mixing protocol, from a local rubber company, is compared with our mixing method.

Differential Scanning Calorimetry

A Netzsch DSC 200 PC instrument, with data acquisition and control, was used to measure the glass transition temperature, T_g, the curing reaction peak and the cure kinetics. Dynamic

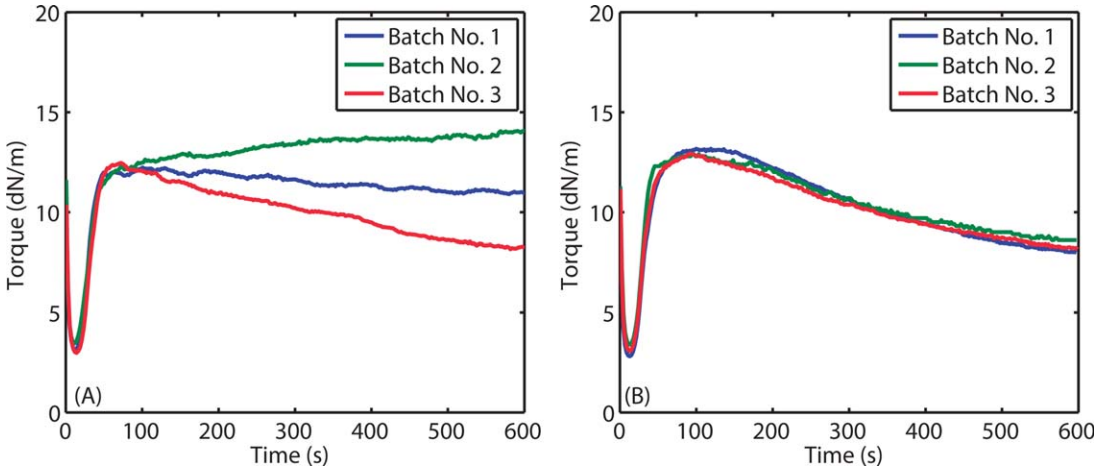

Figure 1. Comparison of torque for various mixing protocols used in the EPDM rubber. (A) Results for a typical industrial mixing protocol; (B) Results for our mixing method. [Color figure can be viewed in the online issue, which is available at wileyonlinelibrary.com.]

and dynamic/isothermal ramps are used. The instrument is operated with a nitrogen flow rate of 20 mL/min through the cell, where an empty pan is used as a reference. For the dynamic experiments, samples between 9 and 12 mg were placed inside aluminum pans and heated to 300 °C using four different heating rates: 1, 2.5, 5, and 10 °C/min. To obtain the $T_{g,0}$ (glass transition temperature at zero conversion), the sample was cooled to −100 °C at a rate of 2.5 °C/min and heated to 25 °C at the same rate. $T_{g,0}$ is identified as an inflection in the baseline using the midpoint method.

To capture the diffusion-controlled mechanism, dynamic/isothermal ramps are performed.[8,9] In this scan, the samples are heated to a specific curing temperature using a low rate of 5 °C/min. This temperature is held for 3 h. After curing, each specimen is heated again to 300 °C to ensure a complete transformation and the process is repeated to obtain the baseline of the experiment. The isothermal curing was performed at three different temperatures: 130, 140, and 150 °C. The DSC data were analyzed using the Netzsch DSC analysis software (Proteus). The baseline obtained in the second run of the dynamic/isothermal experiment and it is subtracted from the first run to find the real reaction peak. Details of the dynamic/isothermal DSC experiments can be found in previous works developed in our group.[8,9] The OBSH decomposition kinetics is measured using a mass between 4.5 and 6.5 mg. Four different heating rates are used for the dynamic scans: 1, 2.5, 5, and 10 °C/min.

Thermogravimetric Analysis

The change in mass during the OBSH decomposition reaction was measured using a thermogravimetric analysis (TGA) Q50 thermogravimetric analyzer from TA Instruments. The samples are evenly and loosely distributed in an open sample pan with an initial sample amount of 8–10 mg. The temperature change was controlled from room temperature (20 °C) to 300 °C at 10 °C/min. A high purity nitrogen stream was continuously passed into the furnace at a flow rate of 50 mL/min. The data analysis was made using the Proteus Analyzer and TA Universal Software.

Rheometric Analysis

The viscosity measurements were done on an Advance Rheometric Expansion System from TA Instruments. Cylindrical samples of 25-mm diameter and 5-mm height were placed between the parallel plates. The experiment was made in a dynamic strain sweep at a frequency of 10 Hz and at three different temperatures: 130, 140, and 150 °C. The duration of the experiments was 15 min. The data were analyzed using the TA Analysis Software (Orchestrator). Even though 1 Hz is also suggested for a dynamic time strain sweep, no reliable results were obtained.

Kinetical and Rheological Models

The DSC and rheometric experiments provide the degree of cure c, curing kinetics, dc/dt, and the viscosity, η, as a function of time and temperature. The kinetics is modeled following the Kamal–Sourour (KS) model while the Castro–Macosko (CM) model is used for the viscosity. These models are not the central aim of the proposed methodology or the chemorheological diagram; they were chosen due to their applicability and their simplicity.[7–9,19–22] It is important to highlight, however, that because these models are phenomenological, their fitting parameters lack physical interpretation. The validity of the results is given by the range of temperatures, pressures, and rates done to characterize the compound. Better models, suitable for particular resins or chemistries, can be included in the methodology to follow particular kinetics or personal preferences.

For completeness, we include the generalities of the auto-catalytic KS model[23,24]; it is defined as follows:

$$\frac{dc}{dt} = (k_1 + k_2 c^m)(1-c)^n, \quad (1)$$

where m and n are the orders of reaction, c is the degree of cure, and k_i are rate constants, described by Arrhenius expressions. Similar to many thermosetting and elastomeric resins, the EPDM vulcanization kinetics is controlled by diffusion at constant temperatures. Therefore, the rate constants, k_i, are modified to include this mechanism, that is[25]:

$$\frac{1}{k_i}=\frac{1}{k_{i,c}}+\frac{1}{k_d}, \tag{2}$$

where $k_{i,c}$ are the Arrhenius dependent rate constants

$$k_{i,c}=a_i\ \exp\left(-\frac{E_i}{RT}\right), \tag{3}$$

and k_d is the diffusion rate constant

$$k_d=a_d\ \exp\left(-\frac{E_d}{RT}\right)\exp\left(-\frac{b}{f}\right). \tag{4}$$

In eqs. (3) and (4), a_i, a_d, and b are adjustable parameters, E_i and E_d are reaction and diffusion activation energies, and f is the equilibrium fractional free volume given by

$$f=0.0048\left(T-T_g\right)+0.025, \tag{5}$$

where T_g is the instantaneous glass transition temperature during cure. For $k_d \gg k_{i,c}$, which is the case prior to vitrification, the overall rate constant is governed by the Arrhenius rate constant, and for $k_d \gg k_{i,c}$, which is the case after vitrification, the overall rate constant is governed by the diffusion rate constant.

Finally, the glass transition temperature, as a function of the conversion, is modeled through DiBenedetto's equation[26]

$$T_g=T_{g,0}+\frac{\left(T_{g,1}-T_{g,0}\right)\lambda c}{1-(1-\lambda)c}, \tag{6}$$

where $T_{g,0}$ is the glass transition temperature of the non-vulcanizated rubber, $T_{g,1}$ is the glass transition temperature of the fully reacted network, and λ is a structure dependent parameter, defined by $\lambda = \Delta C_{p,1}/\Delta C_{p,0}$, where ΔC_p is the difference in heat capacity between the glassy and rubber state for each state of vulcanization.

The rheological behavior is affected by pressure, time, shear rate, filler properties, and temperature. An increase in temperature causes a decrease in viscosity at a given molecular weight. However, as the reaction proceeds, the molecular weight increases, driving an increase in the viscosity.[27] The CM model[12,13,28] is used to capture this behavior, that is,

$$\eta=A\ \exp\left(\frac{E}{RT}\right)\left[\frac{c_g}{c_g-c}\right]^{c_1+c_2\cdot c} \tag{7}$$

where A is a frequency factor, E is the activation energy, R is the universal gas constant, c_1 and c_2 are constants, and c_g is the gel point.

Numerical Methodology

The parameters for the KS and the CM models are fitted to the experimental data via a non-linear least-squares method.[25,29] Hernández-Ortiz and Osswald[12] developed a numerical methodology for polymeric resins that lack diffusion-controlled kinetic mechanisms.[10,13,30] To incorporate diffusion mechanisms, the dynamic/isothermal DSC ramp was introduced.[7–9] It provides the proper experimental setup to capture the different reaction regimens. Previous fitting experiences had determined that the numerical parameters are a function of temperature.[7–11,30] Therefore, a polynomial expansion for each parameter is proposed where the polynomial coefficients are the new targets of the numerical minimization. Hernández-Ortiz and Osswald[13,30] and Lopez *et al.*[10] realized that this fitting process is improved when physically relevant activation energy was obtained directly from the measurements. Therefore, the first activation energy, E_1, in the KS model is obtained by following the Kissinger method,[31,32] being the only physical parameter in the current application.[7–9] The remaining parameters are the final target for the numerical minimization, expressed by a temperature dependent polynomial as follows:

$$x_i = a_{i1}+a_{i2}T\ +a_{i3}T^2+O\left(T^3\right) \tag{8}$$

where $\mathrm{x}=(\boldsymbol{m},\boldsymbol{n},\boldsymbol{a}_1,\boldsymbol{a}_2,\boldsymbol{E}_2,\boldsymbol{a_d},\boldsymbol{b},\boldsymbol{A},\boldsymbol{c}_1,\boldsymbol{c}_2,\boldsymbol{E})$ and the components, a_{ij}, of a matrix $\boldsymbol{A}$ are the numerical minimization target. According to this polynomial expression, the higher terms in the expansion are neglected; accordingly, the fitting must be performed in such a way that the coefficients accompanying the second-order term are small. If this condition is not satisfied for a specific set of data, the expansion cannot assure that the higher order terms are small; consequently, higher order terms must be included in the expansion (i.e., third, fourth). Numerical details of the fitting methodology and the integration scheme can be found in our previous studies.[7,8]

RESULTS

OBSH and EPDM Kinetics

The kinetics of the blowing agent OBSH and the EPDM compound was done carefully in our previous works.[8,33,34] For completeness, we are including the summary of the results and model parameters.

Figure 2 shows the decomposition rate and the cure degree of the OBSH as a function of temperature for different DSC heating scans. These results are for a mixed OBSH that includes the rubber system and reaction modifiers (following an industrial formulation). The total heat of decomposition is Q_T = 776.67 J/g. The reaction decomposition of the OBSH occurs between 120 and 180 °C. The function of the reaction modifiers during the decomposition of OBSH is to diminish the explosive-like reaction of pure OBSH, to broaden the temperature range and to decrease the exothermic peak of the reaction.[33,34] We use the auto-catalytic KM model to model the decomposition reaction of the OBSH. Figure 2 shows the results for the model and all kinetic parameters are listed in Table II.

From dynamic DSC experiments a total heat of vulcanization for the EPDM system $Q_T = 6.6 \pm 0.677$ J/g was measured.[8] The EPDM vulcanization and OBSH decomposition reactions are exothermic reactions and it is reasonable to think that several reaction events will be present during processing. However, we observed a single reaction that indicates a synergy between the vulcanization system and the foaming agent.[8] Recall that, to obtain a good foamed product, a delicate balance between vulcanization and foaming is necessary. For instance, if the curing degree is high, the bubbles generated by the blowing agent cannot grow, but if the vulcanization degree is low, there will not be enough resistance and the gas will diffuse through the rubber.

The value of $T_{g,0}=-55.3$ °C was also measured directly from the dynamic DSC experiment. The glass transition temperature as a function of the cure degree is obtained from the dynamic/isothermal

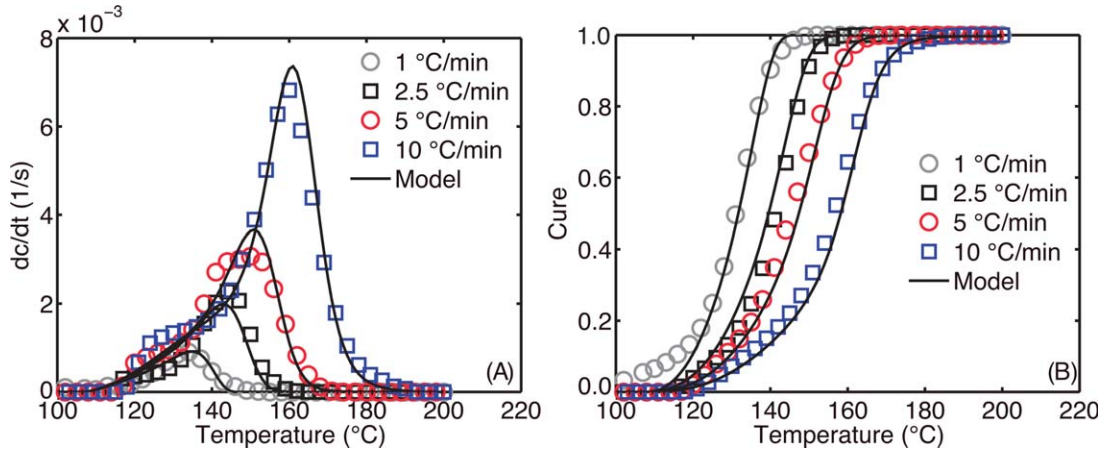

Figure 2. Dynamic DSC fittings for the OBSH decomposition with curing and rubber systems: (A) rate and (B) decomposition degree.[33] [WorldCat]. [Color figure can be viewed in the online issue, which is available at wileyonlinelibrary.com.]

Table II. Kamal–Sourour Model Constants Obtained in Dynamic Experiments for OBSH with Curing and Rubber Systems[33]

Parameter	Value	Units
a_1	$-1.38 \times 10^{15} + 6.61 \times 10^{12}T - 7.81 \times 10^{9}T^2$	s^1
E_1	1.20×10^5	kJ/mol
a_2	$-2.2 \times 10^1 + 1.10 \times 10^{-1}T - 1.36 \times 10^{-3}T^2$	s^{-1}
E_2	6.30×10^3	kJ/mol
M	$2.20 \times 10^2 - 1.04 \times 10^{0}T + 1.24 \times 10^{-3}T^2$	—
N	$-6.90 \times 10^1 + 3.11 \times 10^{-1}T - 3.47 \times 10^{-4}T^2$	—

ramps. The cure degree is calculated as the ratio between the released heat during the dynamic/isothermal ramp and the total heat of reaction, that is, the temperature during the isothermal stage is the glass transition value for that specific released heat. For 130, 140, and 150 °C, the cure were 0.56, 0.84, and 0.93, respectively. The values for λ and $T_{g,1}$ in DiBenedetto's equation are obtained following a non-linear regression fit.[7–9,13] In particular, for the EPDM system, the fitted values for λ and $T_{g,1}$ are 7.37 and 152.1 °C, respectively.

Figure 3 shows the vulcanization (cure) rate and the degree of vulcanization (cure) for the EPDM compound, including diffusion-controlled mechanisms. The figure includes the experimental ramps and the numerical model. The absolute error in the fitting was 1.10×10^{-6}. Table III lists the values for the polynomial coefficients for each kinetic parameter. The dynamic/isothermal experiments indicate that, at later stages, the reaction is controlled by diffusion. Figure 3(B) also shows

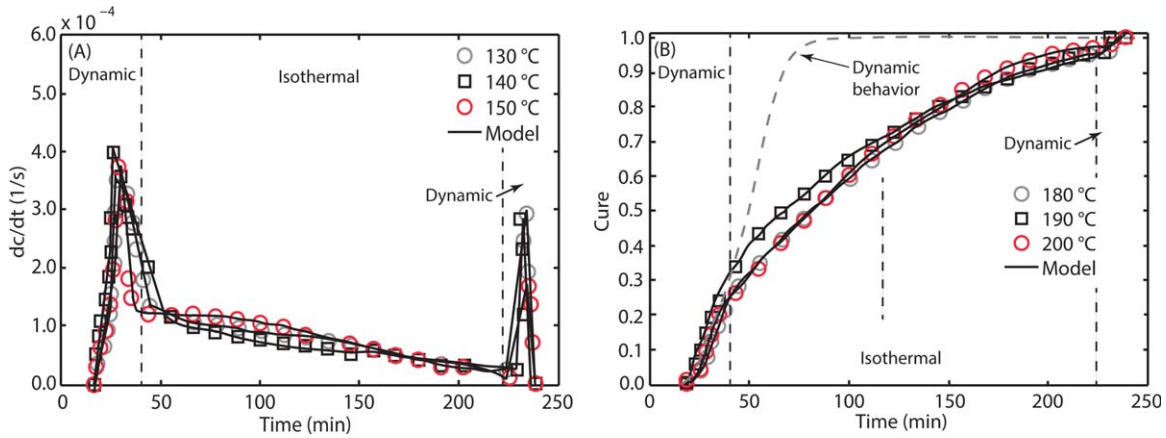

Figure 3. Dynamic/isothermal DSC fitting for the EPDM compound: (A) vulcanization (cure) rate; (B) vulcanization (cure) degree, a comparison with the dynamic behavior of the vulcanization is presented. In these experiments, the diffusion-controlled reaction mechanism are captured and modeled. [Color figure can be viewed in the online issue, which is available at wileyonlinelibrary.com.]

Table III. Kamal–Sourour Model Constants Modified with Diffusion Parameters Obtained with the Dynamic/Isothermal Experiments for the EPDM Compound

Parameter	Value	Units
a_1	$2.66 \times 10^{21} - 1.26 \times 10^{19}T + 1.50 \times 10^{16}T^2$	s^1
E_1	1.73×10^5	kJ/mol
a_2	$3.02 \times 10^{-10} - 1.43 \times 10^{-12}T + 1.70 \times 10^{-15}T^2$	s^{-1}
E_2	-6.45×10^4	kJ/mol
M	$-3.28 \times 10^2 + 1.72 \times 10^0T - 2.26 \times 10^{-3}T^2$	—
N	$3.58 \times 10^2 - 1.68 \times 10^0T + 1.98 \times 10^{-3}T^2$	—
λ	7.37	—
B	$-1.61 \times 10^2 + 7.36 \times 10^{-1}T - 2.24 \times 10^{-4}T^2$	—
a_d	$2.63 \times 10^{-1} - 1.27 \times 10^{-3}T + 1.52 \times 10^{-6}T^2$	—
E_d	-1.40×10^1	kJ/mol

the dynamic behavior of cure at 5 °C/min and the difference with the dynamic/isothermal experiments is remarkable. At the beginning of the reaction, there is a rate increase corresponding to the dynamical part of the experiment (both cures overlap). After that, the rate slowly decreases during the isothermal part of the experiment; meanwhile, the rate of the dynamic cure remains constant until it reaches the total curing. Note that the rate decreases continuously, while the cure degree is far from total conversion. During additional dynamic ramps, a final reaction peak, representing the remaining curing reaction, appears, confirming that the reaction was quenched due to vitrification and diffusion effects. Depending on the temperature of the experiment, the intensity of the last peak decreases due to the lower concentration of unreacted components. It is during the isothermal part that the diffusion-controlled mechanism is capture by the model.

Rheological Model

Figure 4 summarizes the viscosity measurements and the CM model at 130, 140, and 150 °C. To fit the CM parameters, the DSC, TGA, and rheometry data are combined into the kinetic and rheological models to obtain the variation of viscosity with the degree of cure. Similar to the kinetics modeling, the parameters in the CM model are found by a non-linear least square method developed by Hernandez-Ortiz and Osswald.[12] The total fitting error was 6.57×10^{-9}. Table IV lists the values for the fitted polynomial coefficients of the CM model. Notice that, as the reaction progresses, there is an increase in the viscosity and once the cure reaches the gel point, $c_g = 0.647$, the viscosity becomes infinitely large. At the early stages of the reaction, the viscosity decreases due to the increasing temperature. As chemical bonds are generated, the three-dimensional network starts to be formed and the viscosity increases exponentially. It is important to highlight that the rheological experiments provide data of viscosity as a function of time. These results are shown in Figure 4(A). The KS model (i.e., DSC and TGA information) is then used to obtain the viscosity as a function of cure [as shown in Figure 4(B)]. It is, therefore, a great achivement of these phenomenological models to be able to collapse viscosity as a function of the conversion in a single curve at different isothermal conditions. Even more interesting is the fact that these models, the KS and CM, are able to predict a gel point of $c_g = 0.647$, a value that has been predicted by different theories and experiments.[35–37] We believe that this result serves as a mean to validate our methodology.

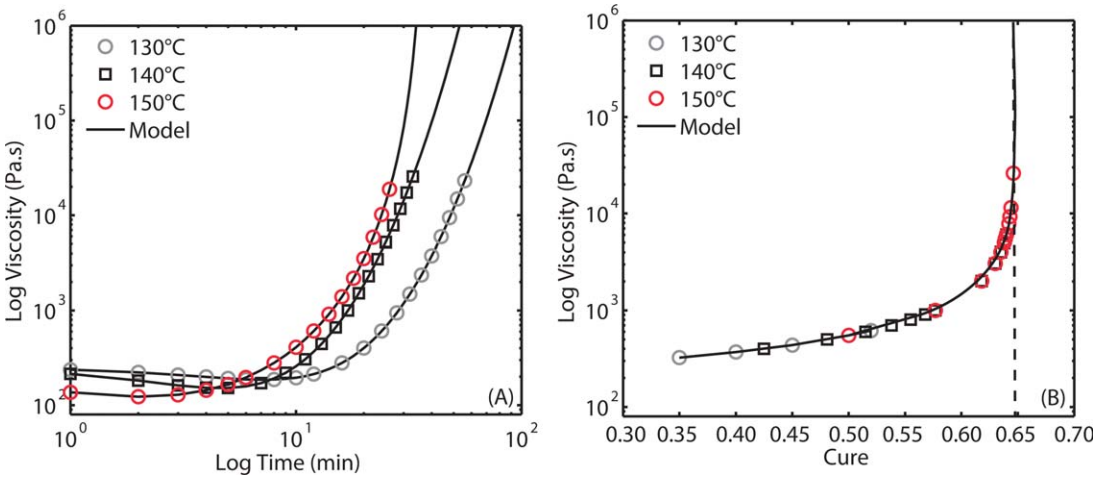

Figure 4. EPDM rubber viscosity as a function of (A) time during vulcanization, using a parallel plate rheometer, and (B) cure degree following the CM model. [Color figure can be viewed in the online issue, which is available at wileyonlinelibrary.com.]

Table IV. Castro–Macosko Model Constants Obtained Using the Rheological Experiments

Parameter	Value	Units
η_o	9.45×10^0	Pa s
E	1.05×10^4	kJ/mol
c_{gel}	0.647	—
c_1	$2.45 \times 10^{-1} + 1.97 \times 10^{-5}\,T + 1.40 \times 10^{-8} T^2$	—
c_2	$7.4 \times 10^{-1} + 3.35 \times 10^{-6}\,T + 4.84 \times 10^{-8} T^2$	—

Chemorheological TTT-η Diagram

The results of the vulcanization kinetics and the rheological analysis are summarized in the chemorheological TTT-η diagram (Figure 5). To generate the diagram, the phenomenological models are numerically integrated during 50,000 h at constant temperature. The "processing" time that is required to reach a specific value of viscosity is recorded.

From the "iso-viscosity" and the vitrification line, the "processability window" for our EPDM compound is delimited. Figure 5(B) shows a zoomed segment of the TTT-η diagram, where proper processing conditions can be estimated. These are defined according to the limits for temperature and time at which the EPDM compound may be processed adequately. At the gelation line (green in Figure 5, $c_g = 0.647$), the tridimensional molecular network reaches a crucial point where a change in the physical state of the EPDM induces an exponential increase of the viscosity (see Figure 4). For temperatures between 142 °C and $T_{g,1} = 152.1$ °C, the gel point is reached before vitrification. After the vitrification line (blue in Figure 5), there is an asymptotical reduction in the reaction rate given by the diffusion-controlled crosslinking. The relative position between gelation and vitrification will provide the correct regimens to process the foamed resin. Notice that at 142 °C, gelation crosses vitrification. This transition temperature is one of the major results obtained by our methodology[22,27,38] because it delimits the control kinetics and the type of process. For instance, gelation is only achieved by a "slow" diffusion-controlled mechanism when the compound is processed below 142 °C and the resin behaves as a viscous fluid (finite viscosity). Therefore, bubbles may increase their size freely, which may induce bubble collapse. Conversely, for temperatures higher than 142 °C, gelation is always achieved by "fast" chemical kinetics and the viscosity is always infinite before reaching vitrification. The interplay between time-temperature and foaming will provide the optimal conditions to reach a uniform cure and bubble distribution. Notice that, for 142 °C, the time required to reach vitrification (gelation) is around 50 min. It places a limit on the required time to reach acceptable conditions and delineates the conditions for post-curing. As the processing temperature is increased, the "gelation" time decreases and the "vitrification" time increases [at 142 °C, there is a change in the curvature of the vitrification line, see Figure 5(B)]. The ratio between gelation and vitrification times, above 142 °C, provides a tool for control and optimization. If post-cure is available, there is no reason to process the foamed resin after gelation is reached, thereby saving processing time. If post-cure is not desired, the correct temperature and time may be extracted from the diagram depending on the desired final cure degree.

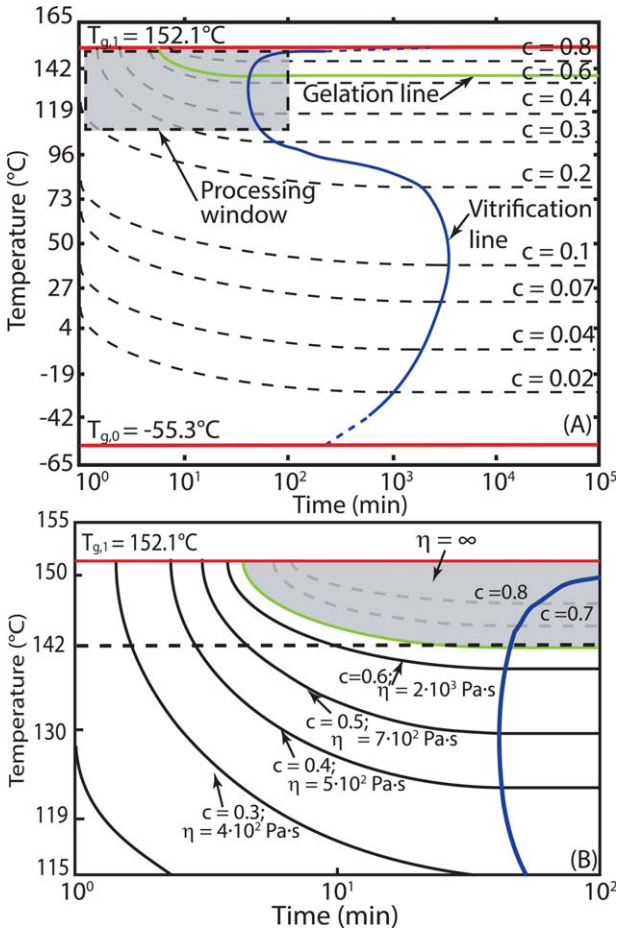

Figure 5. Chemorheological TTT-η diagram: (A) Complete diagram for the EPDM rubber; (B) Operation window including iso-viscosity curves. [Color figure can be viewed in the online issue, which is available at wileyonlinelibrary.com.]

CONCLUSIONS

The chemorheological TTT-η diagram is built based on the results of thermal analysis and rheological experiments. Phenomenological modeling is used for both cure kinetics and rheology. This type of modeling is selected due to their successful application in previous studies, but it does not limit the proposed methodology to any other type of modeling. Cure and viscosity are then condensed in the chemorheological diagram that delineates proper conditions and transitions for optimal processing. The proposed methodology can be used to determine the TTT-η diagram for reactive polymer, that is, thermosets and rubbers.

An industrial-like EPDM rubber compound with a chemical blowing agent is used to illustrate the methodology and chemorheological diagram. For this particular selection, the reaction control starts with a proper mixing methodology and the additional modeling of the blowing agent kinetics. Even though there are additional additives, simultaneous reactions, and complex chemistry, the methodology provided a consistent and comprehensive diagram. Our methodology provides vital information from the resin and compound; for instance, it provides the cure degree at gelation and the transition temperature where the gelation and vitrification balance.

The information from the chemorheological diagram, with the corresponding kinetics and rheology, provides the required information for a complete design and optimization protocols. Computational fluid mechanics and transport may use this information as constitutive equations and kinetics.

ACKNOWLEDGMENTS

The authors wish to thank the Polymer Engineering Center and the Soft Materials Lab at the University of Wisconsin-Madison for the use of facilities and the measurement instruments. JPH-O and NCR are thankful to COLCIENCIAS and Extrusiones S.A. for the financial support of the co-funded project CT-102-2009, 111-845-422-036. JPH-O would like to thank the Biotechnology Center at the University of Wisconsin-Madison and the Institute for Molecular Engineering at the University of Chicago for their help in the experimental setup and computational resources.

REFERENCES

1. Osswald, T. A.; Menges, G. Materials Science of Polymer Engineers, 3rd ed.; Carl Hanser Verlag, Munich, Germany, **2012**.
2. Bird, R. B.; Armstrong, R. C.; Hassager, O. Dynamics of Polymeric Liquids, 2nd ed.; John Wiley & Sons, New York, USA, **1987**.
3. Hiemenz, P. C.; Lodge, T. P. Polymer Chemistry, 2nd ed.; CRC Press, Boca Raton, FL, USA, **2007**.
4. McQuarrie, D. A. Quantum Chemistry, 2nd ed.; University Science Books, Herdon, VA, USA, **2007**.
5. Andre, M.; Wriggers, P. *Int. J. Solids Struct.* **2005**, *42*, 4758.
6. Enns, J. B.; Gillham, J. K. *J. Appl. Polym. Sci.* **1983**, *28*, 2567.
7. Restrepo-Zapata, N. C.; Osswald, T. A.; Hernandez-Ortiz, J. P. *J. Appl. Polym. Sci.* **2014**, *131*, 40566.
8. Restrepo-Zapata, N. C.; Osswald, T. A.; Hernandez-Ortiz, J. P. *Polym. Eng. Sci.*, **2015**, *55*, 2073.
9. Restrepo-Zapata, N. C.; Osswald, T. A.; Hernandez-Ortiz, J. P. *Rev. Iberoam. Polim.* **2012**, *16*, 245.
10. Lopez, L.; Cosgrove, A.; Hernández-Ortiz, J. P.; Osswald, T. A. *Polym. Eng. Sci.* **2007**, *47*, 675.
11. Hadiprajitno, S.; Hernández-Ortiz, J. P.; Osswald, T. A. SPE-ANTEC 2003; Nashville, TN **2003**.
12. Hernandez-Ortiz, J. P.; Osswald, T. A. *J. Polym. Eng.* **2005**, *25*, 23.
13. Osswald, T. A.; Hernandez-Ortiz, J. P. In Polymer Processing: Modeling and Simulation; Carl Hanser Verlag: Munich, Germany, **2006**.
14. Dealy, J.; Larson, R. In Structure and Rheology of Molten Polymers; Carl Hanser Verlag: Munich, Germany, **2006**.
15. Han, X. PhD Thesis, Ohio State University, **2003**.
16. Wang, B. Q.; Peng, L.; Zhang, Y.; Zhang, Y. X. *Plast. Rubber Compos.* **2006**, *35*, 360.
17. Manas-Zloczower, I. In Mixing and Compounding of Polymers: Theory and Practice, 2nd ed.; Carl Hanser Verlag: Munich, Germany, **2009**.
18. Rauwendaal, C. In Polymer Extrusion, 5th ed.; Carl Hanser Verlag: Munich, Germany, **2014**.
19. Kim, D. S. *J. Appl. Polym. Sci.* **2001**, *80*, 873.
20. Sun, X.; Toth, J.; Lee, L. J. *Polym. Eng. Sci.* **1997**, *37*, 143.
21. Chen, Y. T.; Macosko, C. W. *J. Appl. Polym. Sci.* **1996**, *62*, 567.
22. Texier, C.; Taha, M.; Maazouz, A.; Pascault, J. P. *Polym. Eng. Sci.* **1997**, *37*, 1238.
23. Kamal, M.; Sourour, S. *Polym. Eng. Sci.* **1973**, *13*, 59.
24. Sourour, S.; Kamal, M. *Thermochim. Acta* **1976**, *14*, 41.
25. Levenberg, K. *J. Appl. Math.* **1994**, *2*, 164.
26. DiBenedetto, A. T. *J. Polym. Sci. B: Polym. Phys.* **1987**, *25*, 1947.
27. Lopez, J.; Ramirez, C.; Torres, A.; Abad, M. J.; Barral, L.; Cano, J.; Diez, F. J. *J. Appl. Polym. Sci.* **2002**, *83*, 78.
28. Castro, J. M.; Macosko, C. W. SPE-ANTEC Tech. Pap. **1980**, **26**, 434.
29. Marquardt, D. *J. Soc. Ind. Appl. Math.* **1963**, *11*, 431.
30. Hernández-Ortiz, J. P.; Osswald, T. A. *J. Appl. Polym. Sci.* **2011**, *119*, 1864.
31. Kissinger, H. *J. Res. Natl. Bur. Stand.* **1956**, *52*, 217.
32. Kissinger, H. *Anal. Chem.* **1957**, *29*, 1702.
33. Restrepo-Zapata, N. C.; Osswald, T. A.; Hernández-Ortiz, J. P. *Rubber Fibres Plast.* **2015**, *10*, 60.
34. Restrepo-Zapata, N. C.; Osswald, T. A.; Hernández-Ortiz, J. P. *Gummi Fas. Kunstst.* **2015**, *68*, 536.
35. Lodge, A. S. In An Introduction to Elastomer Molecular Network Theory; Bannatek Press, London, **1999**.
36. Flory, P. J. *J. Am. Chem. Soc.* **1941**, *63*, 3091.
37. Harran, D.; Laudouard, A. *Rheol. Acta* **1985**, *24*, 596.
38. Chan, L.; Nae, H.; Gillham, J. *J. Appl. Polym. Sci.* **1984**, *29*, 3307.